THE JOURNAL OF BIOLOGICAL CHEMISTRY VOL. 286, NO. 47, pp. 40922–40933, November 25, 2011

Calcium-sensing Receptor Modulates Cell Adhesion and Migration via Integrins*[S]

Received for publication, May 31, 2011, and in revised form, September 29, 2011 Published, JBC Papers in Press, October 3, 2011, DOI 10.1074/jbc.M111.265454

Sujeenthar Tharmalingam[‡], Avais M. Daulat[‡], Jordan E. Antflick[‡], Syed M. Ahmed[‡], Edward F. Nemeth[‡], Stephane Angers[‡], Arthur D. Conigrave[§], and David R. Hampson[‡1]

From the [‡]Department of Pharmaceutical Sciences, Leslie Dan Faculty of Pharmacy, University of Toronto, Toronto, Ontario M5S 3M2, Canada and the [§]School of Molecular Bioscience, University of Sydney, Sydney, New South Wales 2006, Australia

Background: The calcium-sensing receptor (CaSR) is a nutrient sensor implicated in cell migration.
Results: The CaSR is present in a signaling complex with β1-containing integrins.
Conclusion: The results demonstrate that an ion-sensing G protein-coupled receptor couples to the integrins to promote cellular adhesion and migration in tumor cells.
Significance: Identifying components of the CaSR signaling complex is important for understanding the role of the CaSR in cancer cell metastasis.

The calcium-sensing receptor (CaSR) is a family C G protein-coupled receptor that is activated by elevated levels of extracellular divalent cations. The CaSR couples to members of the G_q family of G proteins, and in the endocrine system this receptor is instrumental in regulating the release of parathyroid hormone from the parathyroid gland and calcitonin from thyroid cells. Here, we demonstrate that in medullary thyroid carcinoma cells, the CaSR promotes cellular adhesion and migration via coupling to members of the integrin family of extracellular matrix-binding proteins. Immunopurification and mass spectrometry, co-immunoprecipitation, and co-localization studies showed that the CaSR and β1-containing integrins are components of a macromolecular protein complex. In fibronectin-based cell adhesion and migration assays, the CaSR-positive allosteric modulator NPS R-568 induced a concentration-dependent increase in cell adhesion and migration; both of these effects were blocked by a specific CaSR-negative allosteric modulator. These effects were mediated by integrins because they were blocked by a peptide inhibitor of integrin binding to fibronectin and β1 knockdown experiments. An analysis of intracellular signaling pathways revealed a key role for CaSR-induced phospholipase C activation and the release of intracellular calcium. These results demonstrate for the first time that an ion-sensing G protein-coupled receptor functionally couples to the integrins and, in conjunction with intracellular calcium release, promotes cellular adhesion and migration in tumor cells. The significance of this interaction is further highlighted by studies implicating the CaSR in cancer metastasis, axonal growth, and stem cell attachment, functions that rely on integrin-mediated cell adhesion.

The calcium-sensing receptor (CaSR)[2] is a widely expressed homodimeric G protein-coupled receptor (GPCR) that functions as a multimodal nutrient sensor to maintain systemic calcium (Ca^{2+}) homeostasis by sensing changes in extracellular Ca^{2+} concentrations. This receptor belongs to a subset of GPCRs (class C) that includes the metabotropic glutamate receptors, the γ-aminobutyric acid, type B receptor, and GPRC6A (1). The CaSR regulates the blood-mineral ion balance largely by regulating parathyroid hormone secretion by the parathyroid gland, calcitonin secretion by the thyroid gland, Ca^{2+} excretion by the kidneys, and osteoblast proliferation and differentiation (2–4). In addition to activation by Ca^{2+} ions, the CaSR is also activated or potentiated by a variety of compounds, including other di- and trivalent cations, polyamines such as spermine, aminoglycosides, as well as other physiologically relevant molecules including L-amino acids and γ-glutamyl peptides (including glutathione), and pharmacologically important phenylalkylamine calcimimetics such as cinacalcet and NPS R-568 (1, 5–8).

The widespread expression of the CaSR in tissues with functions unrelated to plasma Ca^{2+} regulation suggests that the CaSR regulates a variety of processes independent of systemic Ca^{2+} homeostasis. In the nervous system for example, the CaSR has been shown to mediate axonal growth and neuronal branching (9) and to promote spontaneous release of glutamate from nerve terminals (10). CaSR stimulation also induces plasma membrane ruffling (11), and inhibition of CaSR function in stem cells results in defective target localization (11–13).

A role for the CaSR in cell adherence is also supported by studies conducted on hematopoietic stem cells. During fetal development, stem cells from fetal liver migrate to the endosteal surfaces of the bone marrow cavity to undergo hematopoiesis (14). Several studies have demonstrated that the endosteal surface provides a niche for CaSR-expressing hematopoietic stem cells to preferentially localize to the bone and

* This work was supported by the Natural Sciences and Engineering Research Council of Canada and by the National Health and Medical Research Council of Australia.
[S] The on-line version of this article (available at http://www.jbc.org) contains supplemental Figs. 1–3 and Table 1.
[1] To whom correspondence should be addressed: Dept. of Pharmaceutical Sciences, University of Toronto, 144 College St., Toronto, Ontario M5S 3M2, Canada. Tel.: 416-978-4494; Fax: 416-978-8511; E-mail: d.hampson@utoronto.ca.

[2] The abbreviations used are: CaSR, calcium-sensing receptor; ECM, extracellular matrix; GPCR, G protein-coupled receptor; PLC, phospholipase C; rMTC, rat medullary thyroid; IP_3, inositol 1,4,5-trisphosphate; ROCK, Rho kinase; BAPTA, 1,2-bis(2-aminophenoxy)ethane-*N*,*N*,*N*′,*N*′-tetraacetic acid.

that hematopoietic stem cells prepared from mice lacking the CaSR were defective in localizing to the endosteal niche due to defective adhesion to the extracellular matrix protein, type I collagen (12, 13). Finally, a potential role of the CaSR in tumor metastasis is suggested by studies showing the expression of the CaSR in prostate and breast cancer cells that preferentially metastasize to bone (15, 16) and that the elevated Ca^{2+} concentrations detected by the CaSR on highly metastatic, bone-preferring cancer cells have been shown to provide a strong chemo-attractant factor for cancer cell metastasis to bone cells (15, 17).

Despite a large cohort of studies on CaSR function, the signaling partners and protein-protein interactions of the CaSR mediating these effects have not been well characterized. To address this gap, we investigated the signaling proteins and underlying mechanisms involved in CaSR-mediated cell adhesion and migration in rat medullary thyroid carcinoma cells (rMTC 44-2). These metastatic neuroendocrine cells, which endogenously express the CaSR, possess both neuronal and cancerous characteristics (18, 19) and therefore have the potential to serve as a suitable model system to delineate CaSR protein-protein interactions involved in cell adhesion and/or migration.

In initial immunopurification and proteomic analysis experiments of the CaSR, we discovered that the CaSR and β1-containing integrins are present in a macromolecular protein complex in rMTC 44-2 cells. Integrins, which are obligate heterodimers composed of α and β subunits, bind to extracellular matrix (ECM) proteins and function as adhesion proteins that provide cells with a functional link between the intracellular cytoskeleton and the extracellular environment (20, 21). Further analyses using the ECM protein fibronectin in cell adhesion and migration assays revealed that a CaSR-selective positive allosteric positive modulator (NPS R-568) potentiated integrin-mediated cell attachment and migration toward a fibronectin matrix, and both processes are dependent on activation of phospholipase C (PLC) and release in intracellular calcium ($[Ca^{2+}]_i$). Our results reveal that a sequence of events in carcinoma cells that is initiated by increased extracellular Ca^{2+} and followed by the stimulation of the CaSR and release of $[Ca^{2+}]_i$ induces activation of integrins to promote cell adherence and migration.

EXPERIMENTAL PROCEDURES

Membrane Preparation, Solubilization, and Immunopurification—rMTC 44-2 cells were grown in DMEM supplemented with 15% heat-inactivated horse serum and 1.4% GlutaMAX™ in 5% CO_2 at 37 °C. All cell culture reagents were purchased from Invitrogen unless otherwise stated. All immunopurification procedures were performed at 4 °C in the presence of a protease inhibitor mixture (Sigma). rMTC cells grown to 80–90% confluency on 10 150 × 25-mm dishes were isolated and lysed in 10 ml of 50 mM Tris-HCl (pH 7.4) using a Polytron (setting 6, 5 s), followed by centrifugation for 20 min at 48,000 × *g*. The supernatant was removed, and the pellet was resuspended in 5 ml of 50 mM Tris-HCl (pH 7.4). An aliquot of the suspension was used to determine the protein concentration using the Quanti-Pro BCA kit (Sigma), and the remaining suspension was centrifuged for 20 min at 48,000 × *g*. The supernatant was discarded, and the pellet was resuspended in solubilization buffer (50 mM Tris-HCl, 150 mM NaCl, 1 mM $NaH_2PO_4 \cdot 7H_2O$, 10 mM $CaCl_2$, and 1% Triton X-100 (pH 7.5)) at a protein concentration of 3 mg/ml. In some experiments (see under "Results"), the membranes were solubilized with 0.5% CHAPS or 0.5% deoxycholate + 0.1% SDS. The suspension was incubated at 4 °C for 1 h, followed by centrifugation for 1 h at 48,000 × *g*. The supernatant containing the solubilized proteins was collected and aliquoted into 1-ml fractions.

The general procedure for immunoprecipitation was conducted as described previously (22). Briefly, the solubilized samples were precleared with 50 μl of 50% protein A and G slurry (1:1 bead slurry; BioShop) per 1-ml aliquot and incubated for 1 h at 4 °C with rocking. The samples were centrifuged at 2000 × *g* for 2 min, and the pre-cleared supernatant was transferred to a new microcentrifuge tube with 1 μg of anti-CaSR ADD mouse monoclonal antibody (Thermo Scientific Inc., catalog no. MA1-934), 2 μg of anti-CaSR 4640 rabbit polyclonal antibody, or 2 μg of anti-CaSR 4641 rabbit polyclonal antibody (generated in two different rabbits in house at NPS Pharmaceuticals to the ADD sequence ADDDYGRPGIEKFREEAEERDIC), or 2 μg of N-terminal β1 integrin rat monoclonal antibody (AIIB2, Hybridoma Bank), or 2 μg of β1 integrin C-terminal rabbit polyclonal antibody (Chemicon, AB1952) for 1 h at 4 °C rocking. In parallel, protein A + G beads were blocked with 1 mg/ml bovine serum mixture for 1 h, washed, and resuspended in equal volumes of wash buffer (20 mM Tris-HCl, 0.1% Triton X-100, 1% glycerol, and 100 mM NaCl (pH 7.5)). 50 μl of the precleared protein A/G slurry were added to the antibody containing solubilized samples and incubated overnight at 4 °C rocking. The protein A/G beads were collected by centrifugation, washed three times in wash buffer, resuspended in 60 μl of 2× sample buffer (4% SDS, 62.5 mM Tris, and 10% glycerol (pH 6.8)) and 100 mM DTT, and incubated at 37 °C for 15 min. The resulting eluates were subjected to SDS-PAGE and Western blotting. For detection of the CaSR, the Western blots were probed with the CaSR ADD antibody, and for detection of the β1 integrin, the blots were probed with β1 integrin antibodies purchased from Cell Signaling (catalog no. 4706). Peptide:*N*-glycosidase F was obtained from New England Biolabs and used according to the manufacturer's instructions.

Mass Spectrometry Sample Preparation and Protein Identification—The CaSR was immunopurified as described above with minor modifications. Briefly, 10 ml of the Triton X-100-solubilized membrane preparation was precleared with 500 μl of 50% protein A/G slurry and incubated with 10 μg of the CaSR ADD antibody with 150 μl of protein A/G overnight at 4 °C with rocking. The protein A/G beads were collected, washed three times in wash buffer, then washed three times in 50 mM ammonium bicarbonate (pH 7.8), and eluted three times in 200 μl of ammonium hydroxide (pH 11.0) at 37 °C for 15 min each. The combined eluates were dried in a SpeedVac (Thermo Scientific Inc.), and the proteins were resuspended in 50 mM ammonium bicarbonate, reduced in 25 mM dithiothreitol, alkylated with 100 mM iodoacetamide (Sigma), and supplemented with 1 mM $CaCl_2$ prior to digestion with 1 μg of sequenced

grade trypsin (Promega, V511) at 37 °C overnight. The resulting peptide mixture was loaded onto a C-12 reverse-phase nanocolumn packed in-house in a pressure bomb, eluted from an HPLC using a 2-h gradient of buffer A (95% acetonitrile, 0.1% trifluoroacetic acid) and buffer B (95% acetonitrile, 5% water, 0.1% trifluoroacetic acid), and subjected to electrospray ionization followed by analysis on a LTQ-XL linear ion trap mass spectrometer (Thermo Scientific). The acquired tandem mass spectra were searched against the rat NCBI sequences using a normalized implementation of the SEQUEST algorithm running on the Sorcerer platform. The resulting peptide sequences identified by SEQUEST were filtered and assembled into protein identifications using peptide and protein prophets (ISB, Seattle) (23).

Immunocytochemistry—rMTC cells were plated on poly-D-lysine-treated glass coverslips and grown for 3 days in normal culture media. On the day of the experiment, the cells were fixed with 4% paraformaldehyde for 15 min, blocked for 30 min using 5% goat serum (nonpermeabilized), and incubated with extracellular epitope binding anti-CaSR ADD antibody (1:500) and rabbit anti-β1 integrin antibody (1:400; Abcam, AB52971) for 1 h. After four 10-min washes with PBS, the cells were incubated with DyLight 488-conjugated goat anti-mouse (catalog no. 115-485146, Jackson ImmunoResearch) and DyLight 549-conjugated goat anti-rabbit secondary antibodies (1:500; catalog no. 711-505152, Jackson ImmunoResearch) for 1 h. The cells were subjected to a final round of four 10-min washes, and the glass coverslips were mounted onto slides using ProLong Gold Antifade (catalog no. P36930, Invitrogen) and viewed using a Zeiss LSM 510 confocal microscope equipped with a ×100 oil immersion lens. Control conditions were performed in parallel without the presence of primary antibodies.

Cell Culture and Intracellular Ca^{2+} Measurements—Confluent rMTC cells were trypsinized and plated on poly-L-ornithine-treated 96-well microtiter plates (catalog no. 3603, Costar) at 150,000 cells/well in normal culture media. After 24 h in culture, cells were equilibrated with Ca^{2+} assay buffer (20 mM HEPES, 146 mM NaCl, 5 mM KCl, 1 mM $MgCl_2$, 0.5 mM $CaCl_2$, 1 mg/ml bovine serum albumin, and 1 mg/ml glucose (pH 7.4)), loaded with 6 μM Ca^{2+}-sensitive fluorescent dye Fluo-4 AM (Invitrogen), and incubated in the dark for 1 h at room temperature (24, 25). The cells were washed three times and incubated with 150 μl of assay buffer for 30 min at room temperature in the dark. $CaCl_2$ and NPS 89636 dissolved in assay buffer were added at various time points, and the resulting fluorescence measurements (relative fluorescence units) were made at room temperature on a FLEXstation scanning fluorometer (Molecular Devices Inc.) at 485 nm excitation and 525 nm emission (515 nm cut-off). GraphPad Prism was used to plot the relative fluorescence unit measurements and calculate the EC_{50} and Hill slope values. All data represented correspond to means ± S.E. from representative experiments performed in triplicate.

ERK1/2 Phosphorylation Assay—Confluent rMTC cells grown on 12-well plates were serum-starved overnight in DMEM/F-12 (1:1) and preincubated for 3 h with ERK assay buffer (20 mM HEPES, 146 mM NaCl, 5 mM KCl, 1 mM $MgCl_2$, 1 mg/ml bovine serum albumin, and 1 mg/ml glucose (pH 7.4)) containing 1.8 mM Ca^{2+}. The cells were then exposed to 0.003% DMSO or 1 μM R-586 for 5 min at 37 °C in the presence and absence of 50 μM PD 98059. Reactions were terminated with ice-cold PBS, and the cells were lysed using ERK lysis buffer (50 mM Tris-HCl, 150 mM NaCl, 10 mM NaF, 50 mM β-glycerophosphate, 0.25 mM sodium orthovanadate, 500 nM okadaic acid, 1% Triton X-100, 0.5% sodium deoxycholate, 0.1% SDS). The contents of the wells were recovered, solubilized for 10 min at 4 °C, and spun at 21,000 × *g* for 10 min. The supernatant was isolated, and the protein concentration was quantified using the QUANTI PrO BCA kit. 8-μg eq of each protein sample were subjected to SDS-PAGE and Western blotting. Anti-ERK1/2 antibody (1:2000) (catalog no. 4370, Cell Signaling) was used for the detection of phosphorylated ERK1/2, and anti-GAPDH antibody (1:80,000) (catalog no. G3895, Sigma) was used as an internal loading control.

Cell Membrane Isolation—Plasma membrane biotinylation was performed using Pierce EZ-Link Sulfo-NHS-SS-Biotin cell surface protein isolation kit according to the manufacturer's instructions with slight modifications (catalog no. 89881, SulfoLink, Pierce). Briefly, confluent rMTC cells were equilibrated with 0.5 mM Ca^{2+} assay buffer for 5 h and stimulated with 10 mM Ca^{2+} for 10 min. The cells were washed with PBS and incubated in the presence of Sulfo-NHS-SS-Biotin in Hanks' balanced salt solution at 4 °C with gentle agitation. After 30 min, the reaction was quenched, and the cells were harvested, lysed, and subjected to a streptavidin-agarose column. Cytoplasmic proteins unexposed to the biotinylation reaction were isolated into the "flow-through" fraction, and cell surface biotinylated proteins were eluted into the "eluate" fraction. The cytoplasmic and cell surface fractions were separated by SDS-PAGE and immunoblotted using various antibodies.

Cell Adhesion Assay—96-Well flat bottom plates coated with various concentrations of fibronectin (catalog no. F1141, Sigma) were washed and blocked with 2% filtered BSA solution for 1 h at room temperature. rMTC cells were dissociated, washed, resuspended in assay buffer (serum-free DMEM supplemented with 20 mM HEPES and 0.1% BSA (pH 7.4)), and incubated at 37 °C in a humidified 5% CO_2 incubator for 20 min to allow the cells to recover from the process of detachment. In parallel, the wells were aspirated, washed, and incubated with 50 μl of 2× DMSO, NPS R-568, or NPS 89636. For inhibition experiments, 50 μl of 2× NPS R-568 was incubated with 2× GRGDSP or 2× GRADSP peptides (EMD Biochemicals Inc.). 50 μl of cells diluted to 2.5×10^5 cells/ml were plated in triplicate and incubated at 37 °C. After 1 h, the cells were washed three times with warm PBS supplemented with 0.2% BSA. For each condition, input-control wells were maintained without washes. The cells were fixed with glutaraldehyde, stained with 0.1% crystal violent, and quantified by measuring the absorbance at 590 nM in a plate reader (PerkinElmer Life Sciences). Absorbance readings from blank wells were used to subtract the background binding of crystal violet to plastic. Cell adhesion was quantified by representing the background-subtracted absorbance readings as a percentage of input. GraphPad Prism was used to plot the % input values and calculate the EC_{50} and Hill slope values. All data represented correspond to means ± S.E. from representative experiments performed in triplicate.

Haptotaxis Cell Migration Assay—The lower surface of the transwell filters (8.0-μm pore size; catalog no. 353097, Falcon) were coated with 10 μg/ml fibronectin overnight at 4 °C. The filters were washed with PBS, and the lower compartment was incubated with normal culture media in the presence of 1 μM NPS R-568 or DMSO control. 75,000 cells suspended in 200 μl of culture media were added to the upper chamber and incubated at 37 °C for 20 h. For inhibition studies, both the upper and lower chambers were incubated with 500 μM GRADSP, 500 μM GRGDSP, or 1 μM NPS 89636. The cells were washed with PBS, fixed with glutaraldehyde, and stained with 0.1% crystal violet for 1 h. The filters were washed, and nonmigratory cells on the upper side of the filters were removed using cotton swabs. Cell migration was quantified by taking eight random images per well using an inverted phase-contrast microscope (Nikon T100) attached with a Canon digital camera. Cells were counted and expressed as % control.

Preparation of shRNA Lentiviral System and Virus Transduction—Short hairpin (sh) interfering RNA constructs were delivered into rMTC cells by lentiviral transductions. shRNAs directed at the β1 integrin were generated by cloning the following oligonucleotides into a second generation lentiviral packaging system (pLKO.1, Addgene) containing an internal ribosome entry site GFP sequence (generated in-house): β1 integrin shRNA 1 forward, 5′-CCGGGCCATTACTATGATTATCCTTCTCGAGAAGGATAATCATAGTAATGGCTTTTTG-3′; β1 integrin shRNA 2 forward, 5′-CCGGGCACGATGTGATGATTTAGAACTCGAGTTCTAAATCATCACATCGTGCTTTTTG-3′; control scrambled shRNA sequence. Lentivirus was produced by transfecting 30–40% confluent monolayers of HEK293T cells in 10-cm plates with VSV-G (4 μg), psPAX2 (6 μg), and shRNAs cloned into pLKO.1-GFP vector (6 μg) by calcium phosphate transfection method (26). Media were changed 16 h post-transfection, and virus was subsequently collected after 24 and 48 h. Target cells were infected at 1:2 dilution of the virus in DMEM + 10% FBS media followed by media replacement after 24 h. Efficiency of viral infection was assessed by monitoring GFP expression (typically >90%), and knockdown of target protein was verified by Western blot analysis.

Data Analysis and Statistical Significance—Data are reported as means ± S.E. and analyzed by *t* test or one-way analysis of variance followed by Tukey's multiple comparison test. Statistical significance was accepted at $p < 0.05$ for all analyses. Concentration-response curves were generated by analyzing the data via a nonlinear regression method (GraphPad Prism). Individual experiments were standardized by normalizing the data to the maximum and minimum values identified by the fitted curves. The normalized data from several experiments were used to generate the final concentration-response curves.

RESULTS

Functional Activity of CaSR in rMTC 44-2 Cells—In parathyroid cells, stimulation of the CaSR activates G_q and PLC and the subsequent release of $[Ca^{2+}]_i$ (27). To establish whether the CaSR endogenously expressed in rMTC 44-2 carcinoma cells is functionally coupled to this downstream signaling pathway, we stimulated the CaSR with its endogenous ligand Ca^{2+} and measured $[Ca^{2+}]_i$. Upon receptor activation, a very large and robust concentration-dependent rise in $[Ca^{2+}]_i$ was detected. The high level of expression of the CaSR in these cells was confirmed by Western blot analysis (see below). Concentration-response analysis of the data revealed an EC_{50} value for Ca^{2+} of 2.5 ± 0.1 mM and Hill slope of 5.5 ± 0.5, similar to those in other cell types (28, 29). To confirm that the extracellular Ca^{2+}-induced rise in $[Ca^{2+}]_i$ was mediated by the CaSR, the selective CaSR antagonist NPS 89636, was used to block the rise in $[Ca^{2+}]_i$ upon stimulation with extracellular Ca^{2+} (30). NPS 89636 exhibited a concentration-dependent inhibition of the rise in $[Ca^{2+}]_i$ induced by exposure to 5 mM Ca^{2+} with an IC_{50} value of 271 ± 37 nM and Hill slope value of −1.7 ± 0.2 (see supplemental Fig. 1). These results demonstrated that the CaSR is functionally coupled to the Ca^{2+} release pathway in rMTC 44-2 cells. The observation that the Hill coefficients for Ca^{2+} and NPS 89636 are greater than 1 is indicative of intrinsic receptor-based cooperativity, as seen in previous studies.

Identification of Integrins as CaSR Interacting Proteins—To identify novel CaSR signaling partners, the endogenous CaSR expressed in rMTC cells was immunoprecipitated and subjected to LC-MS/MS analysis. Activation of the receptor was required for efficient solubilization from rMTC cell membranes. When solubilization buffer containing calcium below the activation threshold was used (less than 1.5 mM), only low amounts of the CaSR were present in the solubilized fraction. In contrast, solubilization buffer containing high Ca^{2+} (10 mM) sufficient for full receptor activation, the CaSR was highly concentrated in the solubilized fraction (see supplemental Fig. 1). The most prominent group of proteins identified in the LC-MS/MS analysis from the initial CaSR immunoaffinity pull-down experiments was the integrin family of ECM-binding proteins. Members of the integrin family were among the most abundant proteins detected in terms of the total number of peptides identified, the percentage of sequence covered, and probabilities of identified peptides corresponding to the predicted proteins. Several isoforms of α and β integrins were identified in the LC-MS/MS analysis (see supplemental Table 1). β1 integrin was selected for further evaluation because it forms obligate heterodimers with several α integrin subunits.

Co-immunoprecipitation experiments were carried out using the solubilized rMTC cell membrane fraction and three anti-CaSR antibodies (ADD, 4640, and 4641), targeting the CaSR extracellular domain, and two different β1 integrin antibodies targeting the C and N termini of β1 integrin. The ADD monoclonal antibody labeled a doublet on Western blots; deglycosylation of the CaSR caused a shift in the relative molecular mass of the upper 130-kDa band to the lower 120-kDa band (Fig. 1*A*). The β1 integrin N-terminal antibody immunoprecipitated the fully glycosylated form of the CaSR (130 kDa, Fig. 1*B*). Conversely, both the CaSR ADD monoclonal antibody and the β1 integrin N-terminal antibody immunoprecipitated the immature 88-kDa form and, to a lesser extent, the mature 130-kDa glycosylated form of β1 integrin (Fig. 1*C*). To further substantiate this co-immunoprecipitation result, two additional CaSR antibodies (rabbit polyclonals 4640 and 4641) and a C-terminal β1 integrin antibody (Chemicon) were used. The

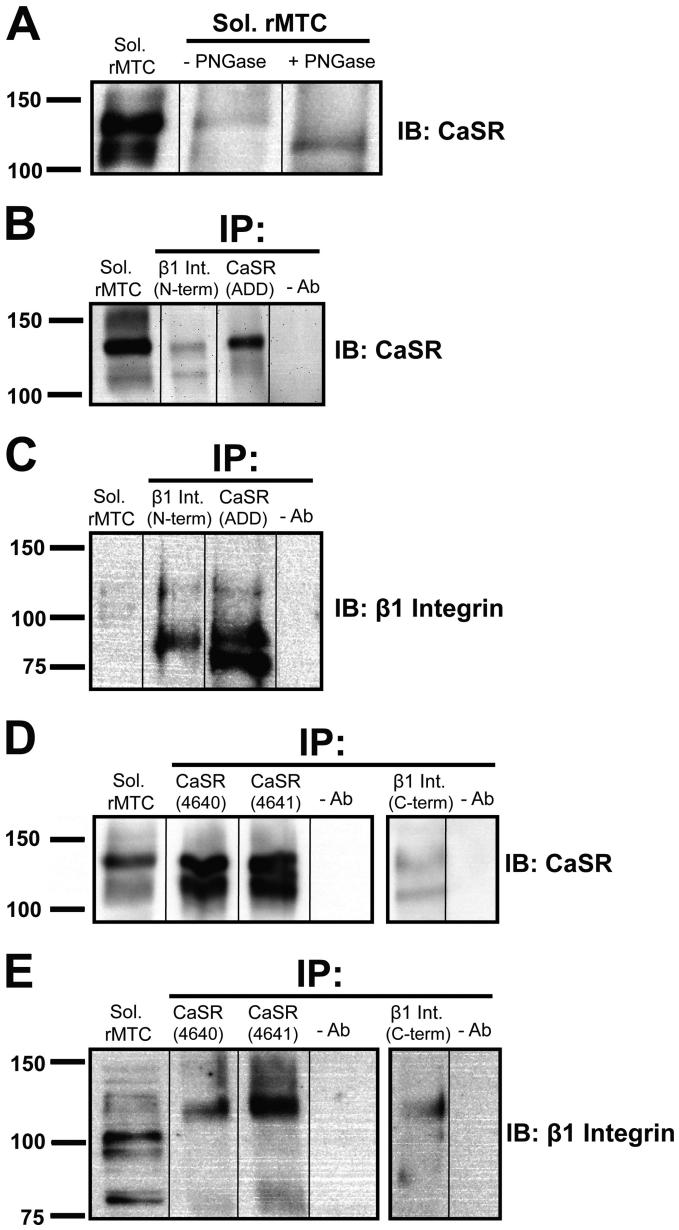

FIGURE 1. **Co-immunoprecipitation (*IP*) of the CaSR and β1 integrin from rMTC 44-2 cells.** Samples of solubilized (*Sol*) rMTC 44-2 cells were immunoprecipitated using three anti-CaSR-specific antibodies (ADD, 4640, or 4641) targeting the extracellular domain of the CaSR and two different antibodies targeting the C or N terminus of β1 integrin. The samples were subjected to immunoblotting (*IB*) using the ADD anti-CaSR monoclonal antibody and anti-β1 integrin antibodies. *A,* deglycosylation of the CaSR with peptide:*N*-glycosidase (*PNGase*) F showing that the upper band in the doublet is the fully glycosylated form of the receptor, and the lower band is the core-glycosylated form; *B* and *C,* co-immunoprecipitation of CaSR and β1 integrin using the CaSR ADD antibody and β1 integrin-specific N-terminal antibody. *D* and *E,* co-immunoprecipitation of CaSR and β1 integrin using CaSR-specific 4640 and 4641 antibodies, and β1 integrin-specific C-terminal antibody. The β1 integrin N-terminal antibody recognized primarily the immature 88-kDa form of the protein (*C*), although the C-terminal β1 antibody recognized primarily the fully glycosylated 130-kDa form (*E*). The blots are representative of two experiments with similar results.

two rabbit polyclonal antibodies strongly immunoprecipitated both the fully glycosylated and core glycosylated forms of the CaSR (Fig. 1*D*), whereas immunoprecipitation with the CaSR ADD monoclonal antibody preferentially immunoprecipitated the fully glycosylated form (Fig. 1*B*). The C-terminal β1 integrin antibody also immunoprecipitated the CaSR (Fig. 1*D*) and immunoprecipitated the mature 130-kDa β1 integrin (Fig. 1*E*), and in samples immunoprecipitated with the 4640 and the 4641 CaSR polyclonal antibodies, the mature 130-kDa form of β1 integrin was also detected when the blots were probed with the anti-β1 integrin antibody (Fig. 1*E*).

To further validate the co-immunoprecipitation results, the rMTC cells were solubilized using more stringent conditions (compared with Triton X-100 only) with either 0.5% CHAPS or 0.5% deoxycholate + 0.1% SDS. Both conditions resulted in solubilization of the CaSR and β1 integrins; more importantly, immunoprecipitation (using the 4641 anti-CaSR antibody) resulted in immunoprecipitation of the CaSR together with the β1 integrins (supplemental Fig. 2). Taken together, the co-immunoprecipitation results of multiple co-immunoprecipitation experiments demonstrated that the CaSR and β1 integrins are present together in a macromolecular complex in rMTC 44-2 cells.

Co-localization and Cell Surface Expression of CaSR and β1 Integrins—The cellular distributions of the CaSR and β1 integrins in rMTC 44-2 cells were assessed in immunolocalization experiments. Cells grown on poly-D-lysine-treated glass coverslips in subthreshold Ca^{2+} levels (1.8 mM) were fixed and incubated with a mouse anti-CaSR monoclonal antibody (ADD) targeting an extracellular epitope and a rabbit anti-β1 integrin antibody (Abcam), and basolateral images were obtained using a confocal microscope. Although no permeabilization reagent was used, we found that fixation of the cells alone caused permeabilization (data not shown). The anti-CaSR antibody revealed an expression pattern of discrete punctate formations throughout the cells (Fig. 2*A*, *green*). Visible puncta of β1 integrin complexes were also abundantly expressed throughout the cell with a distribution similar to that seen with the CaSR (Fig. 2*A*, *red*). In the merged images, the distribution of the CaSR overlapped extensively (but not completely) with that of β1 integrin (Fig. 2*A*, *yellow*). The co-localization was observed at all focal planes (basolateral and apical).

Although the co-localization images suggested that the CaSR and β1 integrins were co-distributed, the membrane locations of the staining were unclear. Therefore, we evaluated cell surface expression of the CaSR and β1 integrins in the presence and absence of CaSR stimulation using a biotin-based cell surface protein isolation method in which biotin-labeled cell surface proteins were immobilized on agarose columns conjugated with streptavidin. To validate this method in rMTC cells, the cell surface-expressed α3 subunit of Na^+/K^+-ATPase was used as a positive control for surface expression, whereas IP_3 receptor expression was used as a negative control to ensure intracellular specific expression. Using this method, the CaSR and β1 integrins were recovered in the cell surface fraction as identified by the presence of the α3 subunit of Na^+/K^+-ATPase, whereas the IP_3 receptor was expressed exclusively in the intracellular fraction (Fig. 2*B*). Some cell surface proteins were also detected at low levels in the intracellular fraction. However, the mature 130-kDa band of the CaSR appeared in the cell surface fraction, whereas the core-glycosylated 120-kDa band appeared in the intracellular fraction (Fig. 2*B*). Quantitation of the cell surface bands among three independent experiments

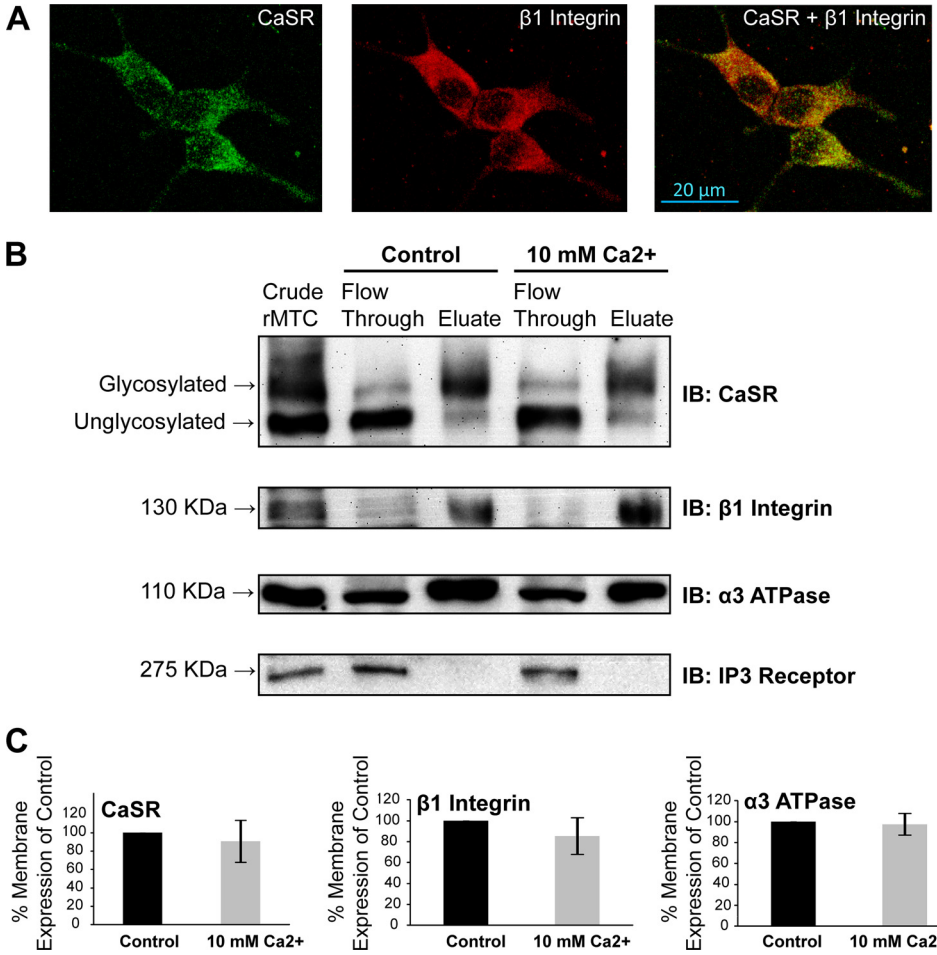

FIGURE 2. **Cellular localization and cell surface expression of the CaSR and β1 integrin in rMTC 44-2 cells.** *A,* cells grown in subthreshold (1.8 mM) Ca^{2+} were immunolabeled with extracellular epitope mouse ADD anti-CaSR antibody (1:500) and a rabbit anti-β1 integrin antibody (1:400) and were viewed using a confocal microscope (×100). CaSR expression was present in discrete puncta distributed throughout the cell (*green*). β1 integrin was also expressed throughout the cell (*red*) and showed extensive overlap with the CaSR expression (*yellow*). Photomicrographs are representative of similar results obtained in three experiments. *B,* cells were preincubated with 0.5 mM Ca^{2+} for 5 h prior to addition of buffer (control) or 10 mM Ca^{2+} for 10 min, and cell surface proteins were covalently biotinylated and subjected to streptavidin-agarose chromatography. Cytoplasmic proteins appeared in the *Flow Through* fraction, whereas cell surface proteins were eluted in the *Eluate*. The CaSR, β1 integrin, and α3 subunits of the Na^+/K^+-ATPase (plasma membrane marker) were found in the cell surface fraction, whereas IP_3 receptor (intracellular membrane marker) was found in the intracellular fractions. The CaSR immunoblot analysis (using the ADD monoclonal antibody) showed that the 130-kDa mature form of the CaSR was recovered primarily in the cell surface fraction as expected, whereas the 120-kDa immature form was recovered in the "flow-through" ($n = 3$). *C,* band intensities present in the eluted fractions of the CaSR, β1 integrin, and α3 subunit blots were analyzed and are presented as a percent of control ($n = 3$).

reveals that the cell surface expression of the CaSR, β1 integrin, and α3 ATPase was not affected by CaSR stimulation (10 mM Ca^{2+}; Fig. 2*C*). Therefore, the biotin-streptavidin affinity chromatography analysis supported the $[Ca^{2+}]_i$ release and immunolocalization studies described above by establishing that both the CaSR and β1 integrins are expressed on the cell surface.

Potentiation of Fibronectin-mediated Cell Adhesion by CaSR-positive Allosteric Modulator—Evidence from LC-MS/MS analysis, co-immunoprecipitation, and co-localization studies revealed that the CaSR and β1-containing integrins appeared to be components of a macromolecular protein complex. The β1-containing integrin heterodimers bind to the ECM protein fibronectin. Therefore, fibronectin matrix-based adhesion assays were conducted to determine the effects of CaSR stimulation on integrin-mediated cell adhesion. Because integrins are affected by changes in divalent cation concentration, including Ca^{2+} and Mg^{2+} (31–33), we obviated the use of cations and instead used a CaSR-specific positive allosteric modulator (NPS R-568) in the presence of a submaximal concentration of extracellular Ca^{2+} (1.8 mM). Fibronectin was coated onto 96-well plates at various concentrations (0–15 μg/ml), and equal numbers of cells were then plated in the presence of 0.02% DMSO (vehicle control), 6 μM R-568, and/or 6 μM R-89636. Maximum cell adhesion levels were observed at fibronectin concentrations above 5 μg/ml. NPS R-568 potentiated the effects of fibronectin-mediated cell adhesion (Fig. 3*A*); compared with control, 6 μM R-568 significantly increased cell adhesion at fibronectin concentrations above 5 μg/ml, with the greatest impact observed at 7.5 μg/ml (166.1 ± 10.2% compared with control). Unlike NPS R-568, NPS 89636 alone had no significant effect on cell adhesion (Fig. 3*A*).

The concentration dependence of R-568-stimulated cell adhesion was investigated at 1 and 2.5 μg/ml fibronectin, corresponding to the EC_{20} and EC_{40} values from fibronectin concentration-response experiments (Fig. 3, *B* and *C*). Under these conditions, R-568 stimulated cell adhesion in a concentration-

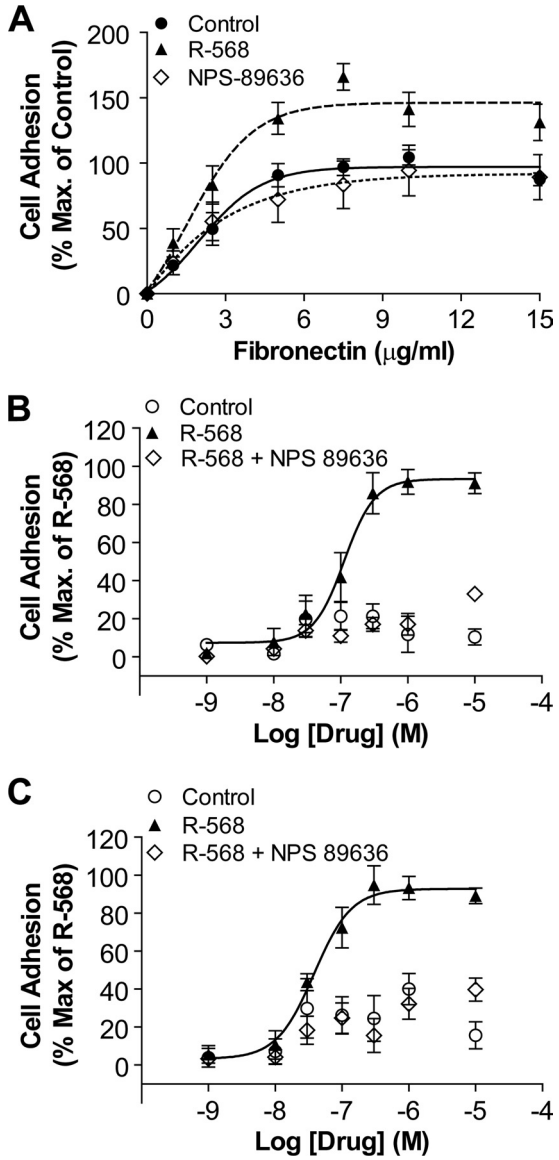

FIGURE 3. **CaSR-positive allosteric modulator NPS R-568 potentiated fibronectin mediated cell adhesion.** *A,* rMTC 44-2 cells were incubated on fibronectin-coated wells (0–15 μg/ml) in the absence or presence of 0.02% DMSO (control), 6 μM NPS R-568, or 6 μM NPS 89636. Treatment of rMTC 44-2 cells with 6 μM NPS R-568 significantly increased cell adhesion over control levels, whereas 6 μM of the CaSR antagonist NPS 89636 did not significantly affect cell adhesion. Each condition from individual experiments was performed in triplicate and expressed as a percentage of "input," which represents control wells that were not subjected to washes. Data points were normalized to maximal cell adhesion level obtained under the control condition (*i.e.* in the absence of R-568 or 89636) ($n = 5$). *B,* NPS R-568 increased cell adhesion in a concentration-dependent manner. rMTC 44-2 cells were incubated on 1 μg/ml fibronectin in the presence of various concentrations of NPS R-568 (1 nM to 10 μM) or DMSO control (3×10^{-6} to 3×10^{-3}%). The data points (mean ± S.E.) were normalized by standardizing basal cell adhesion levels to 0% and maximal adhesion levels to 100% by analyzing the NPS R-568-treated data using GraphPad software. At 1 μg/ml fibronectin, NPS R-568 stimulated cell adhesion in a dose-dependent manner with an EC_{50} = 111 ± 29 nM and Hill slope = 1.9 ± 0.8 ($n = 7$). *C,* at 2.5 μg/ml fibronectin, NPS R-568 displayed a more potent dose-dependent stimulation on cell adhesion, with EC_{50} at 38 ± 12 nM and Hill slope at 1.6 ± 0.5 ($n = 7$). The DMSO vehicle controls showed essentially no effect on cell adhesion.

dependent manner, with an EC_{50} value of 111 ± 29 nM and Hill slope of 1.9 ± 0.8 at 1 μg/ml fibronectin (Fig. 3*B*) and an EC_{50} value of 38 ± 12 nM and Hill slope of 1.6 ± 0.5 at 2.5 μg/ml fibronectin (Fig. 3*C*). Simultaneous addition of NPS R-568 and

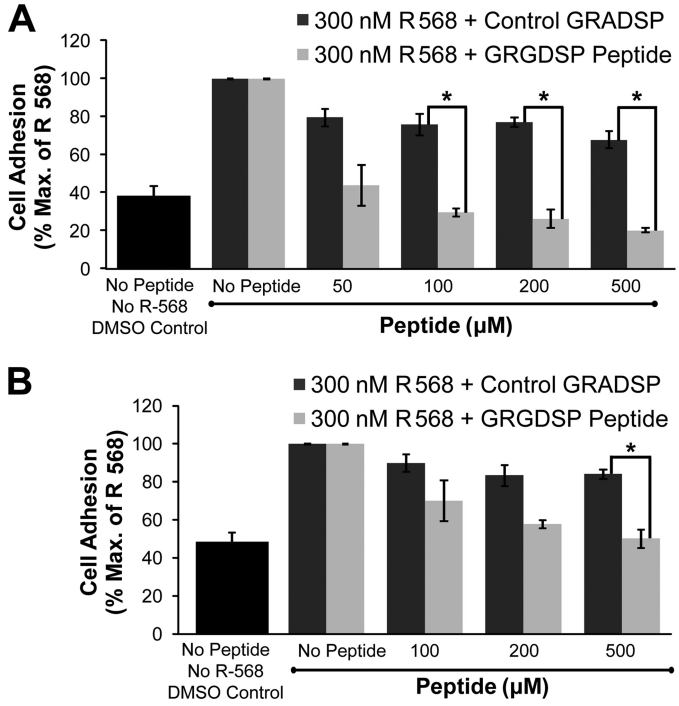

FIGURE 4. **GRGDSP peptide inhibited NPS R-568-mediated cell adhesion.** rMTC 44-2 cells were incubated on 1 μg/ml fibronectin or 2.5 μg/ml fibronectin in the presence of 300 nM R-568 with varying concentrations of the integrin-inhibiting peptide, GRGDSP, or a control peptide, GRADSP, that does not inhibit integrins. *A,* at 1 μg/ml fibronectin, GRGDSP peptide significantly inhibited NPS R-568-mediated cell adhesion at peptide concentrations greater than 100 μM compared with the control GRADSP peptide ($n = 2–4$). *B,* at 2.5 μg/ml fibronectin, 500 μM GRGDSP peptide was required to significantly reduce the potentiation effects of 300 nM NPS R-568 on cell adhesion compared with GRADSP peptide ($n = 4$). The control GRADSP peptide showed a small nonsignificant degree of inhibition on cell adhesion at all concentrations. Data points represent the mean ± S.E. normalized to cell adhesion levels obtained by stimulation with 300 nM NPS R-568 in the absence of peptides. *, $p < 0.05$.

NPS 89636 abolished the effects of NPS R-568 alone (Fig. 3, *B* and *C*). The DMSO vehicle control did not promote cell adhesion at either 1 or 2.5 μg/ml fibronectin. Thus, the CaSR-positive allosteric modulator NPS R-568 potently stimulated rMTC 44-2 cell adhesion in the presence of fibronectin.

Inhibition of NPS R-568-mediated Potentiation of Cell Adhesion by GRGDSP Peptide—The GRGDSP peptide competes with fibronectin for integrin binding and serves as an inhibitor of integrin-mediated cell adhesion on RGD-containing ECM proteins such as fibronectin (21). To investigate whether the effects of R-568 on cell adhesion were dependent on integrin binding to the fibronectin matrix, cell adhesion was measured in the absence or presence of various concentrations of GRGDSP peptide and a single concentration of R-568 (300 nM); as above cells were plated on either 1 or 2.5 μg/ml of the fibronectin matrix. A related peptide GRADSP, which exhibits markedly reduced peptide binding affinity (34, 35), was used as a negative control.

At 1 μg/ml fibronectin, GRGDSP at concentrations at and above 50 μM reduced the stimulatory effect of 300 nM R-568 on cell adhesion in a concentration-dependent manner (Fig. 4*A*). The peptide induced a statistically significant decrease in cell adhesion at concentrations at and above 100 μM compared with the GRADSP control peptide. Thus, 100, 200, and 500 μM

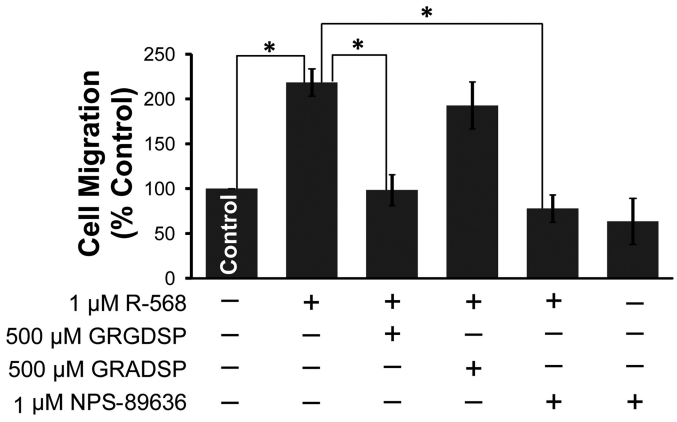

FIGURE 5. **NPS R-568 increased fibronectin-mediated cell migration via integrin activation.** rMTC 44-2 cells added to the upper surface of transwell filters migrated to the lower chamber coated with 10 μg/ml fibronectin. 1 μM NPS R-568 induced a 2-fold increase in cell migration toward the fibronectin matrix as compared with control conditions. The effects of NPS R-568 on cell migration were inhibited in the presence of 500 μM GRGDSP or 1 μM NPS 89636 but not by 500 μM of the GRADSP control peptide. 1 μM NPS 89636 treatment alone did not inhibit cell migration. Each data point represents the mean ± S.E. of 3–6 independent experiments. *, $p < 0.005$.

GRGDSP suppressed cell adhesion by 70.1 ± 2.1, 73.8 ± 4.8, and 79.8 ± 1.3% compared with control no-peptide treatments ($p < 0.05$). At 2.5 μg/ml fibronectin, the GRGDSP peptide inhibited adhesion at concentrations above 100 μM with 500 μM GRGDSP inhibiting 300 nM R-568-mediated cell adhesion by 49.8 ± 6.3% ($n = 4$; $p < 0.05$, Fig. 4*B*). Therefore, GRGDSP inhibited R-568-mediated potentiation of cell adhesion in a concentration-dependent manner. The results demonstrate that CaSR activation potentiates cell adhesion by promoting integrin binding to a fibronectin-rich matrix, at least in part by the RGD peptide sequence present in fibronectin.

R-568 Potentiates Fibronectin-mediated Cell Migration via Integrin Activation—Human forms of medullary thyroid carcinoma are highly metastatic (36, 37). The role of the CaSR-integrin protein complex in cell migration was further investigated in Boyden chamber experiments. rMTC cells did not exhibit chemotaxis in response to various stimuli, including fetal bovine serum, horse serum, or 1 μM R-568. However, rMTC cells displayed directional chemotaxis in response to the ECM protein fibronectin. rMTC cells migrated toward fibronectin matrix-treated filters, whereas no migration was observed in bovine serum-treated filters, and 1 μM R-568 significantly potentiated fibronectin-dependent cell migration by 218 ± 15% compared with a vehicle control (Fig. 5). Furthermore, the potentiating effect of 1 μM R-568 on cell migration was eliminated by 500 μM GRGDSP peptide or 1 μM of the CaSR antagonist NPS 89636, with 98 ± 17 and 77 ± 15% cell migration, respectively ($p < 0.005$). NPS 89636 (1 μM) had no effect on cell migration in the absence of R-568 and the negative control peptide GRADSP did not reverse the positive effect of 1 μM R-568 (Fig. 5).

To further validate the role of β1 integrins in R-568-mediated potentiation of cell adhesion and migration, protein expression levels of β1 integrin in rMTC cells were knocked down by an shRNA lentivirus-based system. Robust protein knockdown was observed using β1 integrin shRNA sequence 2, whereas shRNA sequence 1 showed β1 integrin expression similar to that of the control shRNA (scrambled) condition (Fig. 6*A*). β1 integrin shRNA 2 inhibited R-568-stimulated cell adhesion and migration on fibronectin, whereas scrambled and shRNA 1 treatment did not inhibit CaSR-mediated cell adhesion and migration (Fig. 6, *B* and *C*). These data further demonstrate that CaSR-stimulated cell migration toward a fibronectin matrix is mediated by β1 integrins.

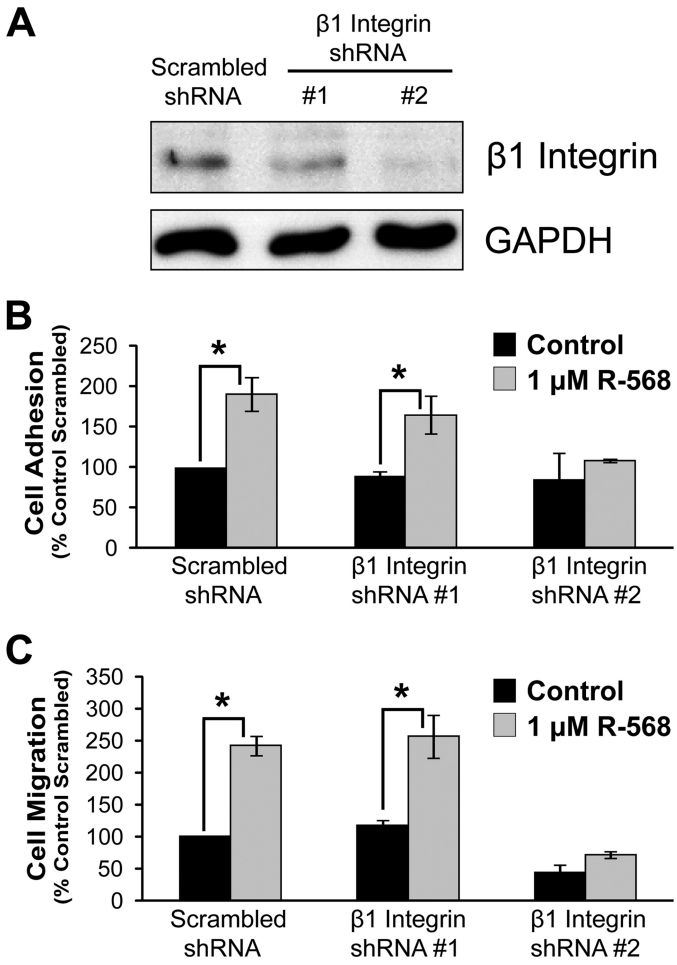

FIGURE 6. **shRNA-mediated knockdown of β1 integrins reduces CaSR-stimulated cell migration.** Cells were treated with one of three shRNA constructs as follows: a scrambled control and two β1 integrins shRNAs *(#1* and *#2*). *A,* Western blot probed with anti-β1 integrin antibody and anti-GAPDH antibody (loading control). *B,* effects of shRNA on cell adhesion (1 μg/ml fibronectin); *C,* effects of shRNA on cell migration (10 μg/ml fibronectin). *B* and *C,* each column is the average ± S.E. of 2–3 experiments. *, $p < 0.05$.

Effects of Intracellular Signaling Inhibitors on CaSR-mediated Cell Adhesion and Migration—CaSR enhancement of cell adhesion and migration could occur through CaSR-mediated intracellular second messenger signaling mechanisms. The CaSR couples to several G protein-dependent signaling systems such as G_q-mediated activation of PLC and $Ca^{2+}{}_i$ release, G_i-mediated reduction in cyclic AMP production, $G_{12/13}$-induced Rho kinase activation, as well as phosphorylation of MAPK/ERK (1, 27, 38–40). These intracellular signaling mechanisms could induce inside-out signaling via an integrin-associated protein to facilitate the binding of integrins to ECM proteins.

To investigate potential biochemical pathways involved in CaSR-mediated cell adhesion and migration, inhibitors of intracellular signaling pathways were tested. It was anticipated that inhibition of the signaling pathway(s) involved in the

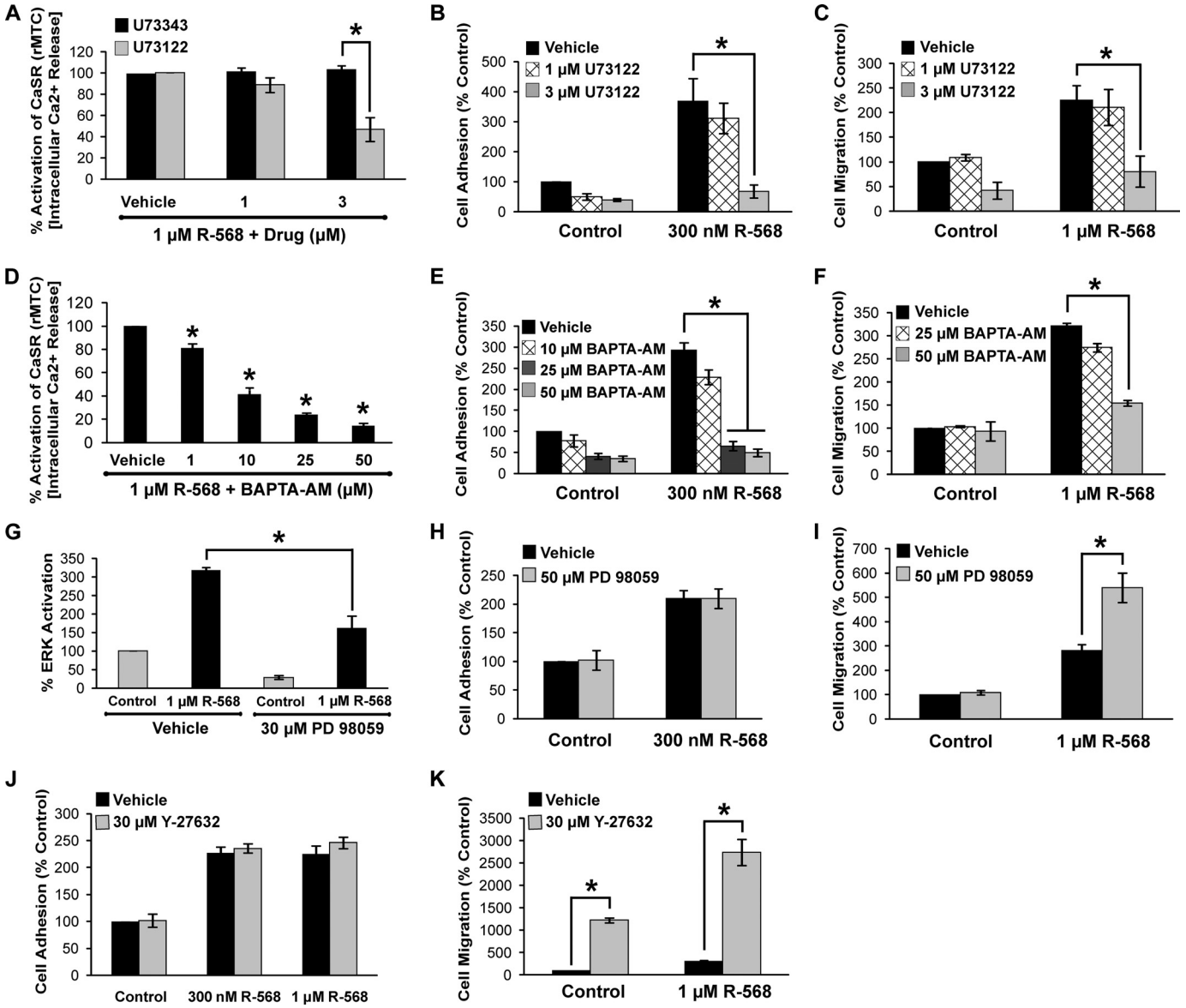

FIGURE 7. **Effects of intracellular signaling inhibitors on Ca^{2+} release, ERK activation, and CaSR-mediated cell adhesion and migration.** *A*, effects of the PLC inhibitor U73122 and the inactive isomer U73343 on CaSR-induced increase in $[Ca^{2+}]_i$. *B*, effects of U73122 on NPS R-568 potentiation of cell adhesion. *C*, effects of U73122 on cell migration. *D*, BAPTA inhibition of $[Ca^{2+}]_i$ release. *E*, effects of BAPTA on NPS R-568 enhancement of cell adhesion. *F*, BAPTA inhibition of the NPS R-568-mediated potentiation of cell migration. *G*, effects of the ERK inhibitor PD 98059 on ERK activation. *H*, effects of PD 98059 on cell adhesion. *I*, PD 98059 enhancement of NPS R-568 potentiation of cell migration. *J*, ROCK inhibitor Y-27632 had no effect on cell adhesion. *K*, effects of Y-27632 on cell migration. Each *bar* represents the mean ± S.E. of 3–5 independent experiments. *, $p < 0.05$.

CaSR-mediated effects would reduce or block CaSR promotion of cell adhesion and migration. Inhibition of $G\alpha_i$, PKC, and voltage-gated calcium channels using pertussis toxin (100 and 200 ng/ml), chelerythrine (5 μM), and verapamil (100 μM), respectively, did not significantly affect NPS R-568 potentiation of cell adhesion or migration (supplemental Fig. 3). In contrast, inhibition of PLC, ERK, and Rho-associated kinase (ROCK) affected CaSR-mediated adhesion and/or migration. The PLC inhibitor U73122 had no significant effect at 1 μM but significantly reduced NPS R-568 stimulation of $[Ca^{2+}]_i$ release and blocked both NPS R-568- potentiated cell adhesion and migration at 3 μM (Fig. 7, *A–C*). Similarly, chelation of $[Ca^{2+}]_i$ with BAPTA-AM significantly reduced the NPS R-568-induced rise in $[Ca^{2+}]_i$ and blocked NPS R-568 potentiation of cell adhesion and migration (Fig. 7, *D–F*).

Inhibition of ERK using PD98059 (30 μM) reduced ERK activation (Fig. 7*G*) but had no effect on basal or NPS R-568-stimulated cell adhesion (Fig. 7*H*). The ROCK inhibitor Y27632 (30 μM) also had no effect on NPS R-568-mediated cell adhesion (Fig. 7*J*). Surprisingly, PD 98059 and Y27632 strongly potentiated the positive effect of NPS R-568 potentiation on cell migration (Fig. 7, *I* and *K*).

In summary, the results of the signal transduction analyses indicated that CaSR stimulation of PLC and the subsequent rise in $[Ca^{2+}]_i$ is required for the positive CaSR effects on cell adhesion and migration.

DISCUSSION

Cell adhesion and migration are crucial events during organogenesis and abnormalities in cell movement and adhe-

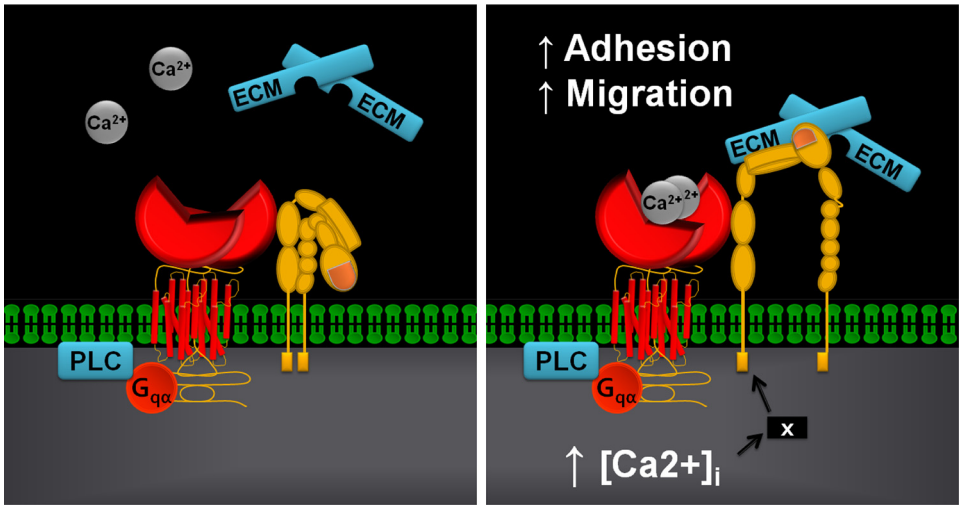

FIGURE 8. **Proposed mechanistic scheme for CaSR-integrin interactions.** The figure depicts one possible scenario where the CaSR may be associated with integrin heterodimers in a signaling complex. However, the actual protein-protein interaction may be indirect and involve additional proteins. *Left*, complex prior to CaSR stimulation; *right*, elevated extracellular cation concentrations activate the CaSR causing its Venus flytrap domain to undergo a conformational change. This protein domain movement together with increased $[Ca^{2+}]_i$ from $G\alpha_q$ activation of PLC and the IP_3 receptor could induce the integrin to flip it into an activated state promoting binding to the ECM resulting in enhanced cell adhesion and migration. The *X* in the *right panel* denotes a hypothetical protein that may participate in facilitating the CaSR-mediated activation of integrins subsequent to increased $[Ca^{2+}]_i$.

sion play an essential role in tumor growth and cancer cell metastasis. Recent studies have implicated the CaSR in the regulation of cell migration in the developing nervous system and in cancer metastasis (9, 15). Here, we identified the integrins as key protein interaction partners with the functionally active CaSR endogenously expressed in rat medullary thyroid carcinoma cells. The integrins are obligate heterodimers composed of α and β subunits. Although there are 18 α and 8 β integrin subunits, only 24 known unique integrin heterodimers have been identified (20). Integrins control cell function by binding to ECM proteins to transduce information from the ECM to adjacent cells, as well as conveying intracellular signals from within cells to the extracellular environment via conferring changes in affinity for ECM proteins. Thus, the integrins display bidirectional signaling and directly participate in various cellular activities involved in cell adhesion and movement (41).

The identification of the integrins as CaSR-interacting proteins was initially determined from CaSR immunoaffinity pull-down experiments in rMTC 44-2 cells (Fig. 1). Further confirmation of the CaSR-integrin interaction was provided by extensive co-immunoprecipitation experiments and cellular co-localization analysis. Pharmacological stimulation of the CaSR using the positive allosteric modulator NPS R-568 potently enhanced cell adhesion and migration. Evidence that these effects occurred via the integrins was provided by the demonstration that the enhancement of cell-ECM adhesion by NPS R-568 could be largely blocked by the addition of GRGDSP integrin-blocking peptide but not by a control peptide (GRADSP) that does not compete with fibronectin for β1 integrin binding. Further confirmation of the role of integrins was obtained in knockdown experiments where shRNA-mediated knockdown of β1-containing integrins reduced CaSR-mediated cell adhesion and migration. We conclude that the CaSR is associated with β1-containing integrins in a macromolecular protein complex and that stimulation of the CaSR promotes cell adhesion and migration via integrin activation.

At the molecular level, potential mechanisms for functional cooperation between the CaSR and integrins include an interaction between the CaSR homodimer and the integrin heterodimers as part of a protein-protein tetramer or, alternatively, in an interaction where the GPCR and integrin are functionally associated indirectly as part of a macromolecular complex containing additional proteins. A calcium-induced conformational change may be followed by a second stage that involves the activation of second messenger-mediated pathways. We propose a model whereby an agonist-induced conformational change in the CaSR induces a shift of the integrin heterodimer into an active conformation (Fig. 8). Both classes of proteins possess large extracellular domains, and although no direct studies examining conformational changes in the CaSR have been reported, other class C GPCRs such as the γ-aminobutyric acid, type B, and the metabotropic glutamate receptors are known to undergo closure of their extracellular Venus flytrap domains upon agonist binding (42–44). A Ca^{2+}-induced stimulation of the CaSR that drives integrins into the active conformation could promote binding to ECM proteins, thereby transmitting conformational changes to other downstream proteins and adjacent cells. Phosphorylation of focal adhesion kinase and subsequent activation of Src kinase is one such pathway by which integrins mediate outside-in signaling (45, 46). These kinases form the backbone of the adhesion and migration complex, and the observation that CaSR can activate Src (47) suggests a possible link between this tyrosine kinase, the CaSR, and integrins in the context of cell adherence.

The results of experiments using inhibitors of intracellular signaling systems demonstrated that activation of PLC participates in CaSR-mediated cell adhesion and migration (Figs. 7 and 8). The PLC inhibitor U73122 and calcium chelator BAPTA were the only signaling pathway inhibitors tested that reduced or blocked the CaSR promotion of cell adhesion and migration. Previous studies have shown that elevated $[Ca^{2+}]_i$, including Ca^{2+}, contributed by the $PLC/IP_3/IP_3$ receptor path-

way, increases cell adhesion and migration (48, 49). Calcium imaging experiments have shown that increased $[Ca^{2+}]_i$ can specify the location and timing of cell process retraction. Moreover, a gradient of $[Ca^{2+}]_i$ that increases toward the rear in migrating cells has been reported (50, 51), and this appears to be linked to Ca^{2+}-dependent cell detachment mechanisms such as increased contractility, enzymatic adhesion disassembly, or increased actin severing to the rear (49, 52, 53). The role of Ca^{2+} in triggering retraction is particularly evident in cells that display transient increases in $[Ca^{2+}]_i$, where Ca^{2+} transients are often observed immediately before a retraction; this process requires the Ca^{2+}-dependent protease calpain (54).

Despite strong evidence for the role of the G_q/PLC/Ca^{2+} pathway described above, we cannot rule out the possibility that the effects may also involve $G_{12/13}$ (and p115 or other RhoGEF-mediated signaling). Because of the inability to transfect the rMTC 44-2 cells, we were not able to test the effects of inhibitory dominant negative cDNA constructs $G_{12/13}$ or RhoGEF in this system.[3]

In addition to the G_q/PLC/IP_3 pathway, we also investigated the ERK and ROCK signaling pathways. In contrast to inhibitors of intracellular calcium release, which reduced or blocked NPS R-568-mediated adhesion and migration, the ERK and ROCK inhibitors had no effect on rMTC 44-2 cell adhesion but *potentiated* the R-568 enhancement of migration. Previous studies examining the effects of ERK and ROCK inhibitors on cell migration have shown variable effects on cell migration. For example, *in vitro* and *in vivo* experiments on breast cancer tissues or cell lines showed that Y27632 inhibited cell migration and metastasis (55), although other studies such as those conducted on trophoblast cells (56) have shown a potentiating effect, as shown here. There is evidence that the effects of ROCK depend on the mode of cell migration (*e.g.* "rounded" *versus* "elongated protrusion" modes of cell motility) in different cell types (57).

Our results with the ERK and ROCK inhibitors were unexpected and differ from some previous reports of the effects of ERK or ROCK on cell migration (58–60). The effect of ROCK inhibition might be due to the fact that ROCK phosphorylates and inactivates myosin phosphatase preventing myosin light chain phosphorylation and subsequent cell outgrowth. Inhibition of ROCK increases neurite outgrowth by preventing the activity of myosin light chain, thereby obstructing F-actin stabilization and actin-myosin cross-linking (61, 62). Thus, destabilization of F-actin promotes stress fiber formation and may have caused increased cell migration in our experiments. In the case of ERK, it has been shown that filamin A binding to the C terminus of the CaSR stabilizes the receptor and attenuates its degradation rate, thereby facilitating MAPK/ERK signaling (63). Our data appear to indicate that CaSR activation of ERK works in opposition to the G_q/PLC/IP_3 pathway in the context of promoting cell migration. We speculate that in rMTC 44-2 cells, the net effect of CaSR stimulation in the absence of signaling inhibitors is the dominance of intracellular calcium release in promoting migration over the inhibitory effect of ERK activation. Further studies are required to fully elucidate the molecular mechanisms mediating the effects of CaSR and ERK on cell migration.

Taken together, our findings reveal that CaSR-expressing cells can participate in cellular mobility by converting an increase in extracellular Ca^{2+} levels into a compartmentalized intracellular Ca^{2+} signal (release from the endoplasmic reticulum via IP_3 receptor activation) that culminates in enhanced cellular movement. Our data suggest that cation-induced protein conformational changes in the CaSR-integrin complex likely operate in conjunction with PLC-mediated $[Ca^{2+}]_i$ release to stimulate the movement of tumor cells.

The rMTC 44-2 cell line was derived from a rat medullary thyroid carcinoma originating from the calcitonin-expressing thyroid C-cells (64, 65). Our results demonstrate that rMTC 44-2 cells express high levels of the CaSR. Human C-cell carcinomas are metastatic and often colonize bone tissue, an environment enriched in extracellular Ca^{2+} at levels sufficient to significantly or fully activate the CaSR. The mechanism of medullary thyroid carcinoma metastasis to bone has never been identified despite clinical data indicating that distant metastasis is observed in 7–23% of patients with medullary thyroid carcinoma cells, and it is a major cause of medullary thyroid carcinoma-related deaths with survival rates of 25% at 5 years after detection and 10% at 10 years (36, 66). Our findings suggest that the CaSR may participate in medullary thyroid carcinoma bone metastasis by activation of a CaSR-integrin signaling complex that becomes preferentially activated in the high Ca^{2+} environment of bone and thereby promoting cellular adhesion of the tumor cells within bone. Breast and prostate tumor cells also metastasize to bone; 65–75% of advanced breast and prostate cancer patients have secondary tumors in bone, with a 5-year survival rate of only 20–25% (67). Interestingly, the CaSR has been shown to enhance the metastatic potential in various bone-preferring breast and prostate cancer cell lines (15, 16, 68). For example, *in vitro* experiments have revealed that blocking CaSR function in PC3 prostate cancer cells and MDA-MB-231 breast cancer cells inhibits cell adhesion and migration (15, 16). Therefore, the key features of the CaSR-integrin complex identified in this study in medullary thyroid carcinoma cells might be applicable to other cancer cell types that robustly express the CaSR and that metastasize to bone.

[3] S. Tharmalingam and D. R. Hampson, unpublished observation.

REFERENCES

1. Conigrave, A. D., and Hampson, D. R. (2010) *Pharmacol. Ther.* **127,** 252–260
2. Brown, E. M. (2000) *Rev. Endocr. Metab. Disord.* **1,** 307–315
3. Riccardi, D., Park, J., Lee, W. S., Gamba, G., Brown, E. M., and Hebert, S. C. (1995) *Proc. Natl. Acad. Sci. U.S.A.* **92,** 131–135
4. Takaoka, S., Yamaguchi, T., Yano, S., Yamauchi, M., and Sugimoto, T. (2010) *Horm. Metab. Res.* **42,** 627–631
5. Conigrave, A. D., Quinn, S. J., and Brown, E. M. (2000) *Proc. Natl. Acad. Sci. U.S.A.* **97,** 4814–4819
6. Nemeth, E. F., Steffey, M. E., Hammerland, L. G., Hung, B. C., Van Wagenen, B. C., DelMar, E. G., and Balandrin, M. F. (1998) *Proc. Natl. Acad. Sci. U.S.A.* **95,** 4040–4045
7. Wang, M., Yao, Y., Kuang, D., and Hampson, D. R. (2006) *J. Biol. Chem.* **281,** 8864–8870
8. Broadhead, G. K., Mun, H. C., Avlani, V. A., Jourdon, O., Church, W. B., Christopoulos, A., Delbridge, L., and Conigrave, A. D. (2011) *J. Biol. Chem.*

286, 8786–8797
9. Vizard, T. N., O'Keeffe, G. W., Gutierrez, H., Kos, C. H., Riccardi, D., and Davies, A. M. (2008) *Nat. Neurosci.* **11,** 285–291
10. Vyleta, N. P., and Smith, S. M. (2011) *J. Neurosci.* **31,** 4593–4606
11. Bouschet, T., Martin, S., Kanamarlapudi, V., Mundell, S., and Henley, J. M. (2007) *J. Cell Sci.* **120,** 2489–2497
12. Adams, G. B., Chabner, K. T., Alley, I. R., Olson, D. P., Szczepiorkowski, Z. M., Poznansky, M. C., Kos, C. H., Pollak, M. R., Brown, E. M., and Scadden, D. T. (2006) *Nature* **439,** 599–603
13. Lam, B. S., Cunningham, C., and Adams, G. B. (2011) *Blood* **117,** 1167–1175
14. Nilsson, S. K., Johnston, H. M., and Coverdale, J. A. (2001) *Blood* **97,** 2293–2299
15. Saidak, Z., Boudot, C., Abdoune, R., Petit, L., Brazier, M., Mentaverri, R., and Kamel, S. (2009) *Exp. Cell Res.* **315,** 2072–2080
16. Liao, J., Schneider, A., Datta, N. S., and McCauley, L. K. (2006) *Cancer Res.* **66,** 9065–9073
17. Saidak, Z., Mentaverri, R., and Brown, E. M. (2009) *Endocr. Rev.* **30,** 178–195
18. Garrett, J. E., Capuano, I. V., Hammerland, L. G., Hung, B. C., Brown, E. M., Hebert, S. C., Nemeth, E. F., and Fuller, F. (1995) *J. Biol. Chem.* **270,** 12919–12925
19. Clark, M. S., Lanigan, T. M., Page, N. M., and Russo, A. F. (1995) *J. Neurosci.* **15,** 6167–6178
20. Luo, B. H., Carman, C. V., and Springer, T. A. (2007) *Annu. Rev. Immunol.* **25,** 619–647
21. Humphries, M. J. (2000) *Biochem. Soc. Trans.* **28,** 311–339
22. Rose, E. M., Koo, J. C., Antflick, J. E., Ahmed, S. M., Angers, S., and Hampson, D. R. (2009) *J. Neurosci.* **29,** 8143–8155
23. Ahmed, S. M., Daulat, A. M., and Angers, S. (2011) *Methods Mol. Biol.* **756,** 357–370
24. Kuang, D., Yao, Y., Wang, M., Pattabiraman, N., Kotra, L. P., and Hampson, D. R. (2003) *J. Biol. Chem.* **278,** 42551–42559
25. Yao, Y., Pattabiraman, N., Michne, W. F., Huang, X. P., and Hampson, D. R. (2003) *J. Neurochem.* **86,** 947–957
26. Ahmed, S. M., Daulat, A. M., Meunier, A., and Angers, S. (2010) *J. Biol. Chem.* **285,** 6538–6551
27. Brown, E. M., and MacLeod, R. J. (2001) *Physiol. Rev.* **81,** 239–297
28. Gama, L., and Breitwieser, G. E. (1998) *J. Biol. Chem.* **273,** 29712–29718
29. Hauache, O. M., Hu, J., Ray, K., Xie, R., Jacobson, K. A., and Spiegel, A. M. (2000) *Endocrinology* **141,** 4156–4163
30. Nemeth, E. F., Delmar, E. G., Heaton, W. L., Miller, M. A., Lambert, L. D., Conklin, R. L., Gowen, M., Gleason, J. G., Bhatnagar, P. K., and Fox, J. (2001) *J. Pharmacol. Exp. Ther.* **299,** 323–331
31. Mould, A. P., Akiyama, S. K., and Humphries, M. J. (1995) *J. Biol. Chem.* **270,** 26270–26277
32. Vorup-Jensen, T., Waldron, T. T., Astrof, N., Shimaoka, M., and Springer, T. A. (2007) *Biochim. Biophys. Acta* **1774,** 1148–1155
33. Puklin-Faucher, E., and Vogel, V. (2009) *J. Biol. Chem.* **284,** 36557–36568
34. Pierschbacher, M. D., and Ruoslahti, E. (1984) *Nature* **309,** 30–33
35. Lin, B., Arai, A. C., Lynch, G., and Gall, C. M. (2003) *J. Neurophysiol.* **89,** 2874–2878
36. Modigliani, E., Cohen, R., Campos, J. M., Conte-Devolx, B., Maes, B., Boneu, A., Schlumberger, M., Bigorgne, J. C., Dumontier, P., Leclerc, L., Corcuff, B., and Guilhem, I. (1998) *Clin. Endocrinol.* **48,** 265–273
37. Moley, J. F., and DeBenedetti, M. K. (1999) *Ann. Surg.* **229,** 880–888
38. Magno, A. L., Ward, B. K., and Ratajczak, T. (2011) *Endocr. Rev.* **32,** 3–30
39. Huang, C., Hujer, K. M., Wu, Z., and Miller, R. T. (2004) *Am. J. Physiol. Cell Physiol.* **286,** C22–C30
40. Davies, S. L., Gibbons, C. E., Vizard, T., and Ward, D. T. (2006) *Am. J. Physiol. Cell Physiol.* **290,** C1543–C1551
41. Barczyk, M., Carracedo, S., and Gullberg, D. (2010) *Cell Tissue Res.* **339,** 269–280
42. Tsuchiya, D., Kunishima, N., Kamiya, N., Jingami, H., and Morikawa, K. (2002) *Proc. Natl. Acad. Sci. U.S.A.* **99,** 2660–2665
43. Pin, J. P., Comps-Agrar, L., Maurel, D., Monnier, C., Rives, M. L., Trinquet, E., Kniazeff, J., Rondard, P., and Prézeau, L. (2009) *J. Physiol.* **587,** 5337–5344
44. Hampson, D. R., Rose, E. M., and Antflick, J. E. (2008) in *The Glutamate Receptors: The Structure of Metabotropic Glutamate Receptors* (Gereau, R. W., and Swanson, G. T., eds) pp. 363–386, Humana Press Inc., Totowa, NJ
45. Mitra, S. K., and Schlaepfer, D. D. (2006) *Curr. Opin. Cell Biol.* **18,** 516–523
46. Mitra, S. K., Hanson, D. A., and Schlaepfer, D. D. (2005) *Nat. Rev. Mol. Cell Biol.* **6,** 56–68
47. McNeil, S. E., Hobson, S. A., Nipper, V., and Rodland, K. D. (1998) *J. Biol. Chem.* **273,** 1114–1120
48. Sjaastad, M. D., Lewis, R. S., and Nelson, W. J. (1996) *Mol. Biol. Cell* **7,** 1025–1041
49. Valeyev, N. V., Downing, A. K., Skorinkin, A. I., Campbell, I. D., and Kotov, N. V. (2006) *In Silico Biol.* **6,** 545–572
50. Brundage, R. A., Fogarty, K. E., Tuft, R. A., and Fay, F. S. (1991) *Science* **254,** 703–706
51. Brust-Mascher, I., and Webb, W. W. (1998) *Biophys. J.* **75,** 1669–1678
52. Doyle, A. D., and Lee, J. (2002) *BioTechniques* **33,** 358–364
53. Wong, R., Fabian, L., Forer, A., and Brill, J. A. (2007) *BMC Cell Biol.* **8,** 15
54. Robles, E., Huttenlocher, A., and Gomez, T. M. (2003) *Neuron* **38,** 597–609
55. Liu, S., Goldstein, R. H., Scepansky, E. M., and Rosenblatt, M. (2009) *Cancer Res.* **69,** 8742–8751
56. Fafet, P., Rebouissou, C., Maudelonde, T., and Vignais, M. L. (2008) *Endocrinology* **149,** 4475–4485
57. Sahai, E., and Marshall, C. J. (2003) *Nat. Cell Biol.* **5,** 711–719
58. Huang, C., Jacobson, K., and Schaller, M. D. (2004) *J. Cell Sci.* **117,** 4619–4628
59. Lester, R. D., Jo, M., Campana, W. M., and Gonias, S. L. (2005) *J. Biol. Chem.* **280,** 39273–39277
60. Zohrabian, V. M., Forzani, B., Chau, Z., Murali, R., and Jhanwar-Uniyal, M. (2009) *Anticancer Res.* **29,** 119–123
61. Lingor, P., Teusch, N., Schwarz, K., Mueller, R., Mack, H., Bähr, M., and Mueller, B. K. (2007) *J. Neurochem.* **103,** 181–189
62. Hirose, M., Ishizaki, T., Watanabe, N., Uehata, M., Kranenburg, O., Moolenaar, W. H., Matsumura, F., Maekawa, M., Bito, H., and Narumiya, S. (1998) *J. Cell Biol.* **141,** 1625–1636
63. Zhang, M., and Breitwieser, G. E. (2005) *J. Biol. Chem.* **280,** 11140–11146
64. Gagel, R. F., Zeytinolu, F. N., Voelkel, E. F., and Tashjian, A. H., Jr. (1980) *Endocrinology* **107,** 516–523
65. Fajtova, V. T., Quinn, S. J., and Brown, E. M. (1991) *Am. J. Physiol.* **261,** E151–E158
66. Bergholm, U., Bergström, R., and Ekbom, A. (1997) *Cancer* **79,** 132–138
67. Coleman, R. E. (1997) *Cancer* **80,** 1588–1594
68. Mamillapalli, R., VanHouten, J., Zawalich, W., and Wysolmerski, J. (2008) *J. Biol. Chem.* **283,** 24435–24447